JOURNAL OF TROPICAL LIFE SCIENCE
2026, Vol. 16, No. 1, 49 – 61
http://dx.doi.org/10.11594/jtls.16.01.05

Research Article

Structural Homology Modelling, Molecular Docking and Initial Insight into Phenol Degradation Activity of Recombinant Tyrosinase from *Lentinula edodes* Mushroom

Viaevanilly David [1], Mohd Nasir Bin Abdul Rasah [1], Herman Umbau Lindang [2], Ruzaidi Azli Mohd Mokhtar [1], Jaya Seelan Sathiya Seelan [3], Rafida Razali [4], Cahyo Budiman [1]*,

[1] Biotechnology Research Institute, Universiti Malaysia Sabah, Kota Kinabalu, 88400 Sabah, Malaysia
[2] Sarawak Tropical Peat Research Institute, Kota Samarahan, 94300 Sarawak, Malaysia
[3] Institute for Tropical Biology and Conservation, Universiti Malaysia Sabah, Kota Kinabalu, 88400 Sabah, Malaysia
[4] Faculty of Science and Resource Technology, Universiti Malaysia Sarawak, Kota Samarahan, 94300 Sarawak, Malaysia

Article history:
Submission October 2025
Revised March 2026
Accepted March 2026

**Corresponding author:*
E-mail: cahyo@ums.edu.my

ABSTRACT
Tyrosinase is a copper-containing enzyme known for ability to degrade phenolic compounds, making it highly attractive for industrial applications, particularly in wastewater decontamination. While fungal tyrosinase is considered an excellent source for enzyme studies and applications, deeper investigations into its structural properties and phenol degradation activity are still needed. This study aims to elucidate the structural properties of tyrosinase from the mushroom *Lentinula edodes* (Edo-Tyr) and evaluate its phenol degradation activity. The amino acid sequence of Edo-Tyr was retrieved from GenBank (AB 033993.1) and used to construct three-dimensional models via Robetta, SWISS-MODEL, and Phyre2. The best model obtained from SWISS-MODEL indicated that the structure is predominantly helical, with a Cu^{2+} ion observed in the active site coordinated by His64, His90, His99, His261, His165, His289, and His290. Structural comparisons revealed similarity between Edo-Tyr and tyrosinase from *Bacillus megaterium* (Bm-Tyr), with an R.M.S.D of 1.38 Å. Sequence alignment further suggested that His265 serves as the active site in Edo-Tyr, analogous to His208 in Bm-Tyr. Molecular docking analysis demonstrated that the catalytic mechanism of Edo-Tyr likely involves hydroxylation via an electrophilic attack, potentially facilitated by a tyrosine rotation event. Key residues implicated in this process include His64, His265, His90, Pro277, and Asp262. Subsequent in vitro assays using a phenol solution confirmed the recombinant Edo-Tyr's ability to degrade phenol, achieving a 48% reduction in phenol concentration with 0.3 U/µL of tyrosinase. These findings confirm the potential application of Edo-Tyr in bioremediation, specifically for phenol decontamination, highlighting its promise for industrial and environmental applications.

Keywords: Lentinula edodes, phenol decontamination, structural homology modeling, tyrosinase

Introduction

Tyrosinase (EC 1.14.18.1), a copper-containing enzyme classified under the polyphenol oxidase family, is pivotal in the biosynthesis of melanin and oxidation of phenolic compounds. This enzyme, found ubiquitously across various life domains, including plants, fungi, bacteria, and animals, tyrosinase contributes to critical biological processes such as pigmentation, UV protection, wound healing, immune responses, and the enzymatic browning of fruits and vegetables [1-3]. Given its broad biological significance, tyrosinase has become a focal point for industrial and environmental applications, such as phenol decontamination and biosensor devel-

How to cite:
David V, Rasah MNBA, Lindang HU, et al. (2026) Structural Homology Modelling, Molecular Docking and Initial Insight into Phenol Degradation Activity of Recombinant Tyrosinase from *Lentinula edodes* Mushroom. Journal of Tropical Life Science 16 (1): 49 – 61. doi: 10.11594/jtls.16.01.05.

opment [4]. Phenol decontamination involves the removal of toxic phenolic compounds from industrial effluents prior to environmental discharge. This is critical as phenols are highly toxic, persistent, and harmful to aquatic ecosystems and human health even at low concentrations. Tyrosinase facilitates this process by oxidizing phenols into quinones, which subsequently polymerize into less toxic, insoluble products that can be removed from wastewater [1,4]. High phenol levels are commonly reported in effluents from petroleum refineries, coal processing, and pulp and paper industries, and accidental releases have caused fish mortality, ecosystem disruption, and contamination of drinking water sources [5-6]. Even concentrations as low as 0.001–0.01 mg/L can render water unsuitable for consumption, emphasizing the need for effective removal strategies such as enzymatic treatment [7]. In addition, tyrosinase is widely utilized in biosensor technologies as a biorecognition element. It catalyzes the oxidation of phenolic substrates at electrode surfaces, generating electroactive quinones that produce measurable currents proportional to phenol concentration. This enables sensitive and selective detection in environmental monitoring, food safety, and clinical screening applications [4]. These applications require a sustainable enzyme supply and a thorough understanding of its catalytic properties to optimize performance under practical conditions [1,4].

Structural studies of tyrosinase are crucial for elucidating catalytic mechanisms and engineering enhanced variants. The core of tyrosinase activity lies in its active site, which contains two copper ions (CuA and CuB) coordinated by histidine residues [8-9]. These copper ions interact with molecular oxygen and phenolic substrates during catalysis, making the active site architecture a key determinant of enzyme functionality. Despite its importance, structural information on mushroom-derived tyrosinase remains limited, with only a few studies available. For instance, tyrosinase structures from *Agaricus bisporus* (common white button mushroom) have been resolved and reveal a conserved copper-binding motif critical for activity [4]. However, structural variations, such as loop regions near the active site or glycosylation patterns, have been reported in tyrosinases from different sources [8,10]. These differences likely influence substrate specificity, catalytic efficiency, and stability, highlighting the need for further structural characterization of tyrosinase from diverse sources.

Among the various mushroom-derived tyrosinases, *Lentinula edodes* (shiitake) presents a particularly compelling subject of study for several reasons. Firstly, it represents an excellent source of tyrosinase due to its natural abundance and ease of cultivation [11]. Secondly, in tropical regions such as Sabah, Malaysia, *L. edodes* is widely consumed and locally known as “kulat jipun” or Borneo mushroom, underscoring its regional availability and socio-economic importance. This local relevance further supports its potential as a practical bioresource for enzyme production and environmental applications within the region [12-13]. Thirdly, this mushroom is a promising source of enzymes with potential biotechnological applications, particularly for phenol decontamination; however, comprehensive fundamental studies are still required to fully support its utilization. Lastly, the structural properties of tyrosinase from *L. edodes* (Edo-Tyr) remain largely unexplored, limiting our understanding of its functional and catalytic mechanisms. This knowledge gap, together with its potential application in phenol bioremediation, makes Edo-Tyr an attractive candidate for further investigation. Previous studies have shown that the catalytic mechanism of tyrosinase involves several key steps, including oxygen binding to the copper ions at the active site, followed by substrate binding, oxidation, and product release [8,14]. Detailed structural studies are therefore essential to elucidate these mechanisms. For instance, structural characterization can reveal how specific substrates, such as L-DOPA, interact with the enzyme, including the roles of surrounding amino acid residues and copper coordination [8]. Additionally, capturing structures of catalytic intermediates may provide insights into the enzyme’s transition between hydroxylase and oxidase activities. Comparative analyses of tyrosinases from different mushroom species may further elucidate how variations in active-site architecture influence catalytic efficiency, stability, and substrate specificity.

Although the structures of tyrosinase from certain mushrooms, such as *A. bisporus*, are well-documented [4], little is known about the unique structural features of Edo-Tyr. This gap significantly limits the exploitation of *L. edodes* as a source of functional enzymes. Moreover, while

recombinant production of Edo-Tyr has been reported, its functional validation, particularly in terms of phenolic compound degradation, remains unconfirmed. This study addresses these limitations by applying computational approaches to investigate the structural properties of Edo-Tyr and evaluate its capacity for phenol degradation. It provides the first evidence of the substrate-binding properties of this protein, highlighting its promising potential for phenolic decontamination.

Material and Methods

Homology structural modeling

The amino acid sequence of tyrosinase was obtained from the complete genome sequence of *L. edodes*. The corresponding gene sequence is available in the NCBI database under accession number AB 033993.1. This nucleotide sequence was utilized to construct a homology model of Tyrosinase through different protein structure prediction platforms, Robetta, SWISS-MODEL and Phyre2. The model was then evaluated and validated according to Global Model Quality Estimation (GMQE), QMEAN statistical parameters, and G factor Procheck. The amino acid sequence of Edo-Tyr was retrieved from the complete genome sequence of *L. edodes.* The corresponding gene sequence is available in the NCBI database under accession number AB 033993.1. The nucleotide sequence was then used for constructing the homology model of Edo-Tyr using the ab initio protein structure prediction server of Robetta [15-18]. The model was then evaluated and validated according to Global Model Quality Estimation (GMQE), QMEAN statistical parameters, and G factor Procheck [19-21].

Molecular docking simulation

The structural model of Edo-Tyr obtained above was used for a molecular docking study as the receptor. Meanwhile, the known substrate for tyrosinase, l-3,4-dihydroxyphenylalanine (L-DOPA), was selected as the ligand. Both receptors and ligands were prepared by minimizing the energy and then 3D protonating in MOE [22]. Further, the docking of the ligand onto PAP was performed using YASARA Structure software (Yet Another Scientific Artificial Reality Application) [23]. Briefly, the receptor and ligand files in .pdb format were used to set the target and play the macro in the YASARA structure software. Then, the docking analyses were performed using the local and global docking default macro file dock_runlocal.mcr and dock_run.mcr, respectively. The macro files were used to calculate the interaction energy (kcal/mol) and dissociation constant, K_D (pm), of the complexes. Meanwhile, local docking was executed by a predefined square grid with a size of 10Å x 10Å x 10Å around the catalytic site of the receptor. Further, the receptor file was saved in.yob format as required for the local docking study. Both local and global docking studies undergo 25 VINA docking runs of the ligand to the receptor. Afterward, the Edo-Tyr complexes were converted into PDB files by YASARA software and visualized for its 2D-3D interactive study with the help of Discovery Studio Visualizer version v19.1.0.18287 (BIOVIA, San Diego, CA, USA) and PyMOL Software. To note, the selection of the area around the catalytic site for the binding site during docking was based on the finding of other tyrosinases, which showed that the substrate docked into this area. The catalytic sites of Edo-Tyr were identified using sequence alignment as detailed below.

Sequence alignment

Sequence alignment of the amino acid sequences was done using T-coffee [24-26]. Before the amino acid Multiple Sequence Alignment (MSA), the sequences were extracted from the Protein Data Bank (PDB) in FASTA format. The MSA was adapted from the constructed multiple sequence alignment by Ozvoldik et al. [22] and Orobitg et al. [23]. The amino acid sequences of tyrosinase from other organisms were retrieved from the PDB, which include *Bacillus megaterium* (Tyr-Bm), *Priestia-megaterium* (Tyr-Pm), *Streptomyces-castaneoglobispor* (Tyr-Strep), *Agaricus bisporus* (Tyr-Ab), *Burkholderia-thailandensis* (Tyr-Bt), *Verrucomicrobium spinosum* (Tyr-Vs) and *Hahella* sp. (Tyr-Ha). The generated file from the T-coffee server was then displayed in a shaded box display using the Boxshade tools in the Expasy server to visualize better the aligned residues [27-28].

Phenol decontamination activity

Recombinant tyrosinase of *L. edodes* was obtained from Haslina Asis of Biotechnology Research Institute, Universiti Malaysia Sabah, which was produced through heterologous ex-

pression under *Escherichia coli* BL21(DE3). The purity of the protein was first examined using 15% SDS-PAGE according to Koshkina et al. [29]. The phenol degradation method was prepared according to [30] with slight modifications. Briefly, a phenol solution was prepared at a concentration of 0.1 mg/mL, as determined from the standard calibration curve. The reaction mixture was prepared in a 20 mM sodium phosphate buffer, pH 6.8, to maintain enzyme stability and activity. The assay was conducted at a controlled temperature of 25°C, and reactions were initiated by the addition of recombinant Tyr-Edo at varying concentrations, ranging from 0 – 2.5 U/mL. The reaction mixtures were incubated for a 60 min period to allow sufficient enzymatic conversion of phenol. Following incubation, the absorbance of residual phenol was measured at 260 nm using distilled water as a blank. The concentration of phenol before and after treatment was quantified based on the calibration curve, and the percentage of phenol removal was calculated accordingly. Experiments were performed in triplicate (n = 3), and data were analyzed using one-way ANOVA followed by Tukey's post hoc test [31-32].

Result and Discussions

The pairwise sequence alignment revealed variable levels of amino acid similarity between Tyr-Edo and tyrosinases from bacterial and fungal origins (Figure 1). The sequence alignment demonstrates notable amino acid similarities, particularly in regions surrounding the conserved histidine residues that coordinate the copper-binding sites. Tyr-Edo shows higher similarity with the fungal tyrosinase from *A. bisporus*, consistent with their evolutionary proximity, while the bacterial sequences exhibit more divergence, especially in the N- and C-terminal regions marked by insertions and deletions. Despite these variations, the conserved blocks of amino acids within the catalytic domains highlight a strong evolutionary constraint to maintain enzymatic function across diverse taxa. Further, Tyr-Edo exhibited the highest sequence identity with *A. bisporus* tyrosinase (Tyr-Ab; 40.83%), suggesting that despite being derived from a distinct source, Tyr-Edo may share partial structural or functional motifs with fungal tyrosinases. In contrast, the similarity with *V. spinosum* (Tyr-Vs; 18.75%), *B. thailandensis* (Tyr-Bt; 24.47%), and *Hahella sp.* (Tyr-Ha; 20.55%) was relatively low, reflecting a distant evolutionary relationship and potential divergence in catalytic or regulatory domains. Among bacterial tyrosinases, Tyr-Edo showed modest conservation with *S. castaneoglobisporus* (Tyr-Strep; 20.91%) and *B. megaterium* (Tyr-Bm; 21.48%). In contrast, Tyr-Bm and *P. megaterium* (Tyr-Pm) displayed exceptionally high sequence identity (95.85%), consistent with their taxonomic proximity, and both exhibited stronger similarity with Tyr-Strep (41.94–42.86%) than with Tyr-Edo. This highlights the evolutionary clustering of *Bacillus/Priestia* tyrosinases, while Tyr-Edo appears to be positioned more distantly.

These observations are consistent with the representative selection of tyrosinases employed in this study, which, although not exhaustive, encompasses key phylogenetic diversity across both fungal and bacterial lineages. Such a balanced dataset provides a robust framework for comparative analysis, enabling the identification of conserved catalytic residues, particularly the histidine motifs involved in copper coordination, alongside variations in peripheral regions that may influence enzyme stability, regulation, or substrate specificity [8]. The inclusion of closely related fungal tyrosinases, such as *A. bisporus*, facilitates the recognition of shared structural and functional features, while the incorporation of more distantly related bacterial counterparts highlights lineage-specific divergence, especially in terminal regions and regulatory domains [33]. This comparative approach not only reinforces the existence of a conserved functional core essential for tyrosinase activity but also reveals evolutionary adaptations that may underlie differences in catalytic efficiency and environmental responsiveness. Collectively, these findings strengthen the positioning of Tyr-Edo within the broader evolutionary landscape of tyrosinases, suggesting that it retains fundamental catalytic characteristics while potentially exhibiting unique properties shaped by its distinct biological origin.

From a functional standpoint, the relatively low overall sequence identity (mostly <25%) between Tyr-Edo and bacterial tyrosinases suggests that Tyr-Edo may represent a novel or divergent tyrosinase variant. Sequence divergence in tyrosinases often corresponds to differences in substrate specificity, catalytic efficiency, and stabil-

ity under environmental conditions [34-35]. The moderate similarity with fungal tyrosinase (Tyr-Ab) could imply that Tyr-Edo retains certain conserved copper-binding or active-site motifs characteristic of the tyrosinase family, but with substantial variation in peripheral or regulatory regions. Such divergence may reflect adaptation to a unique ecological niche, possibly influencing the range of phenolic substrates it can oxidize or its potential utility in biotechnological applications (e.g., bioremediation, biosynthesis of pigments, or antioxidant compounds) [36-37]. These findings suggest that Tyr-Edo is structurally distinct yet evolutionarily anchored within the broader tyrosinase family, with functional potential that warrants further biochemical and structural characterization.

Further, a structural homology model of Edo-

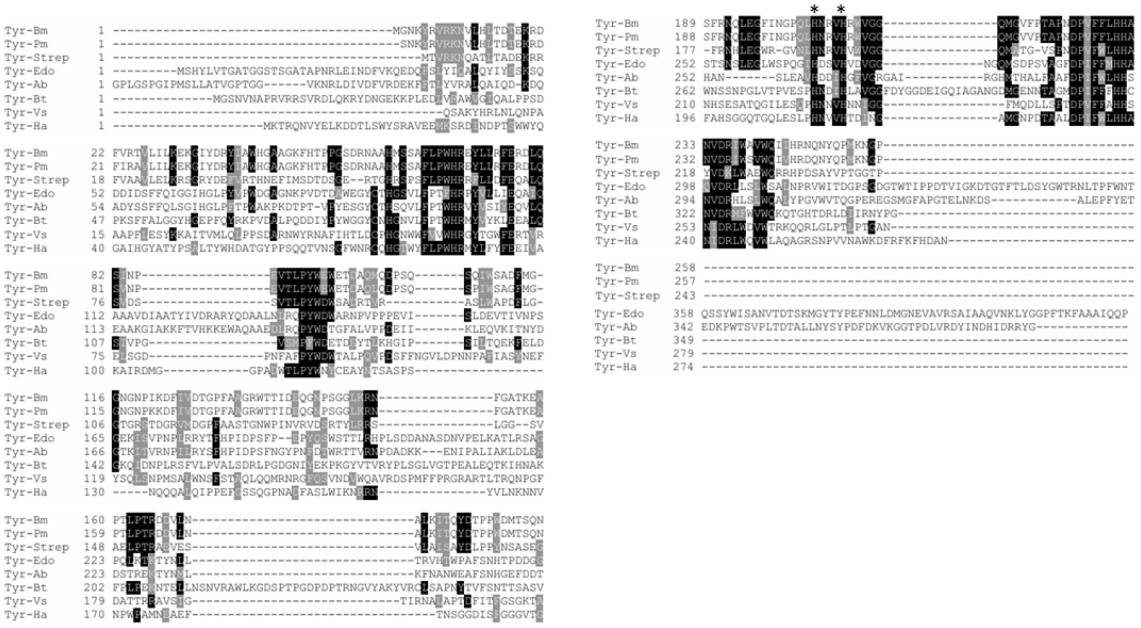

(a)

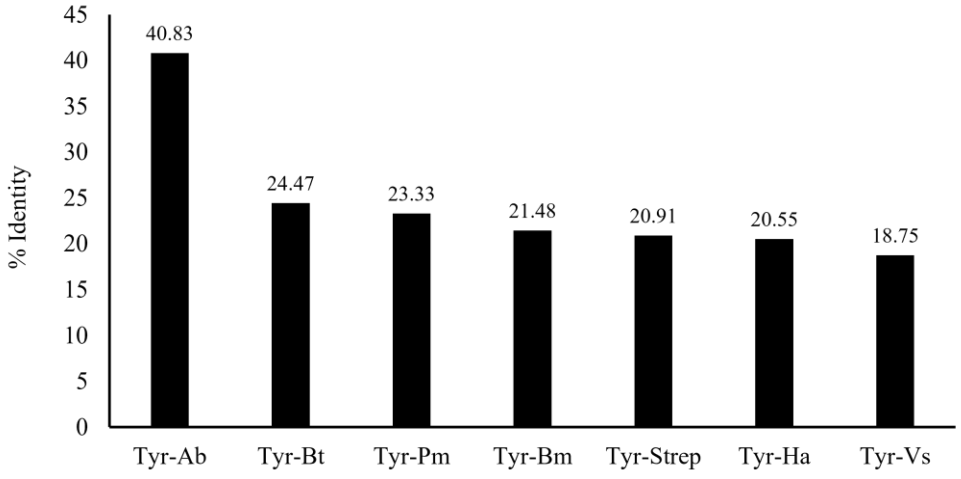

(b)

Figure 1. (a) Multiple sequence alignment and (b) comparison of the percent identity of amino acid sequences of tyrosinases from various sources. Putative active sites are indicated by asterisks (*). The sequences used in the analysis were tyrosinases from *Lentinula edodes* (Tyr-Edo), *Bacillus megaterium* (Tyr-Bm), *Priestia megaterium* (Tyr-Pm), *Streptomyces castaneoglobisporus* (Tyr-Sc), *Agaricus bisporus* (Tyr-Ab), *Burkholderia thailandensis* (Tyr-Bt), *Verrucomicrobium spinosum* (Tyr-Vs), and *Hahella* sp. (Tyr-Ha).

Tyr was constructed using three different platforms of Robetta, SWISS-MODEL, and Phyre2. The consideration of the use of this software is based on the use of different algorithms, which might possibly provide different structural models with different accuracy. Accordingly, the possibility of obtaining the most accurate model will be reliable. The models of each software were obtained and examined with respect to their quality parameters, as shown in Table 1. The assessment parameters include side-chain geometry, dihedral angles, covalent geometry, QMEAN scores, and Ramachandran plot statistics. This comparative analysis highlights the strengths and weaknesses of each server's modeling capabilities. Among the three model servers, shown in Table 1, the structural validation and assessment revealed that the model obtained from the SWISS-MODEL platform exhibited the highest QMEAN score among the other models, which suggests superior overall model quality. The QMEAN score, a composite measure of model quality, reflects the balance between global and local structural accuracy, and a higher score indicates a model that more closely resembles experimentally determined structures. In this regard, SWISS-MODEL (Model 1) demonstrated a robust performance, supported by the highest percentage of residues in the favored regions of the Ramachandran plot (95.42%), a key indicator of correct backbone geometry. This level of structural accuracy is further reinforced by the low percentage of outliers (0.98%), indicating minimal structural errors. Although SWISS-MODEL Edo-Tyr exhibited slightly lower planar group accuracy (90%) compared to Robetta and Phyre2, this discrepancy did not significantly affect the overall model quality. In fact, the slightly reduced planar group accuracy was offset by its superior performance in other parameters, making SWISS-MODEL (Edo-Tyr) a well-rounded tool for general protein modeling tasks. These results suggest that SWISS-MODEL is an optimal choice for applications that require high-quality models with minimal structural deviations across various quality metrics, particularly when a balance between different parameters is desired.

Figure 2a presents the 3D structure of Tyr-Edo, modeled using SWISS-MODEL and visualized with PyMOL. The structure is predominantly composed of helical elements, as depicted in Figure 2a. A total of 11 helices (α1–α11) were identified, with the longest helix (α3) extending from Leu94 to Tyr120. In contrast, two helices, α9 and α10, are relatively short, spanning Gln273–Ser275 and Ala280–Phe282, respectively. The remaining helices are of moderate length, including α1 (Ile25–Tyr46), α2 (Phe57–His64), α4 (Arg125–Asn134), α5 (Pro150–Val152), α6 (Val211–Arg236), α7 (Trp239–Ser243), α8 (Leu258–Val267), and α11 (Ile285–Leu303). Additionally, a beta-hairpin motif was observed, comprising segments Glu157–Asn162 (β1) and Gly165–Pro171 (β1). Similar dominance of helical structures has been reported in other tyrosinases [38-40]. While the functional role of the beta-hairpin motif in tyrosinase has not been extensively detailed, [41] suggested that such structural motifs often contribute to overall structural stability and are involved in various biological functions, including protein-protein interactions.

A model structure notably revealed the pres-

Table 1. Homology Structure Assessment and Validation of Tyr-Edo

Homology Assessment Parameters	Platform Model			
	Robetta	Swiss Model (model 1)	Swiss Model (model 2)	Phyre2
Chi1–chi2[a]	1	2	6	1
Side-chain[a]	5	5	5	5
Cis-Peptides[a]	3	3	2	3
Dihedrals[a]	0.2	-0.13	-0.44	-0.04
Covalent[a]	0.38	-0.01	-0.5	-0.23
Overall[a]	0.28	-0.06	-0.35	0.23
Planar Groups Within Limit (%)[a]	90	90	84.7	100
QMEAN[b]	0.72 ± 0.05	0.76 ± 0.05	0.46 ± 0.05	0.68 ± 0.05
Ramachandran Favoured Region (%)[b]	95.13	95.42	92.09	88.20
Ramachandran Outlier Region (%)[b]	1.30	0.98	1.38	3.61
Ramachandran Allowed Region (%)[c]	5.18	2.94	6.55	9.20

[a] Procheck; [b] SWISS-MODEL Structure Assessment; [c] Zlab Ramachandran Plot Server

ence of a single Cu^{2+} ion (Figure 2b), a characteristic feature of this enzyme essential for its activation [42]. As illustrated in Figure 2, the ion is closely associated with seven histidine (His) residues—His64, His90, His99, His261, His165, His289, and His290—potentially facilitating electrostatic interactions. According to Noh et al. [43] histidine residues play a crucial role in coordinating Cu^{2+} ions in tyrosinases across various organisms. Interestingly, the number of histidine residues involved in Cu^{2+} coordination varies among tyrosinases. For instance, Decker et al. [44] reported six histidine residues coordinating the Cu^{2+} ion in CuA and CuB sites, whereas Noh et al. [43] identified seven histidine residues at the catalytic site of human tyrosinase. Notably, while His289 appears to be within contact distance of the Cu^{2+} ion, its orientation may not favor direct interaction. This raises questions about the role of His289 in anchoring the Cu^{2+} ion, warranting further investigation to clarify its precise function in the coordination process.

Furthermore, superimposition with the well-studied tyrosinase from *B. megaterium* (Bm-Tyr) revealed moderate structural similarity between the two proteins, with an R.M.S.D of 1.38 Å (Figure 2c). Interestingly, sequence alignment, shown in Figure 2b, indicated that His265 in

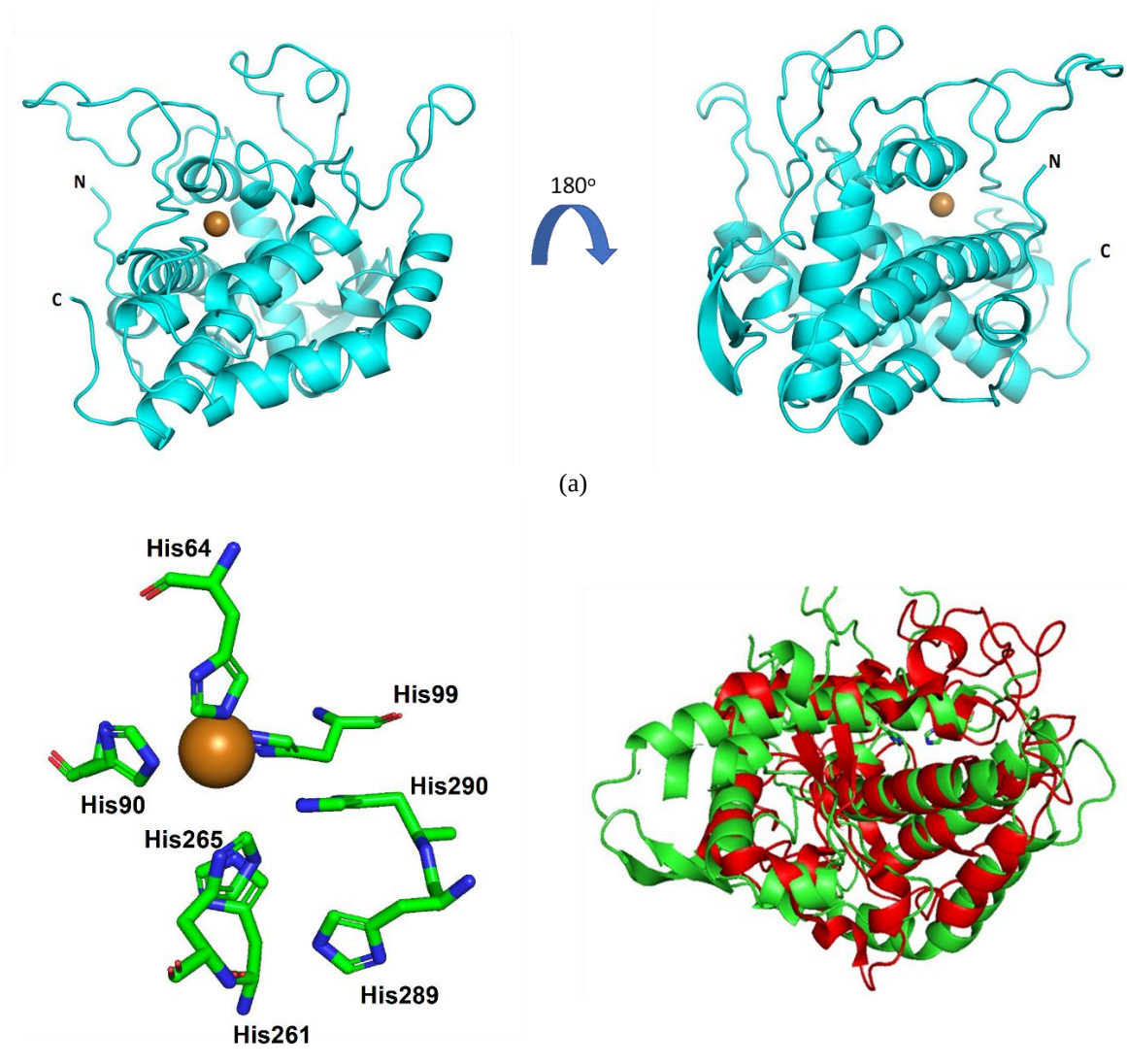

Figure 2. Structural features of Tyr-Edo. (a) Predicted 3D structure showing 11 α-helices and a β-hairpin motif. (b) Active site with a Cu^{2+} ion coordinated by seven histidine residues. (c) Superimposition with Bacillus megaterium tyrosinase (Bm-Tyr) shows moderate similarity (R.M.S.D 1.38 Å) and conservation of His265 as a catalytic residue.

Edo-Tyr is predicted to serve as an active site residue, as it is highly conserved and corresponds to His208 of Bm-Tyr, a known active site residue [10]. As shown in Figure 1b, His265 is also involved in interactions with the Cu^{2+} ion, aligning well with findings by Oyama et al. [39], which confirmed that Cu^{2+} is located within the active sites of tyrosinases.

Molecular docking simulations with L-DOPA demonstrated that Edo-Tyr establishes multiple stabilizing interactions with the substrate, most notably through hydrogen bonding with His64, His265, and Asp262 (Figure 3). These residues are highly conserved in tyrosinases across both fungal and bacterial lineages and are crucial for coordinating the dicopper active center. The positioning of His265 near the O1 hydroxyl group of L-DOPA closely resembles the interaction reported for His208 in *B. megaterium* tyrosinase (Bm-Tyr), where it stabilizes the phenolic oxygen during catalytic turnover [10, 45-46]. This structural similarity suggests that Edo-Tyr follows a mechanistic pathway analogous to Bm-Tyr, where oxidation occurs through the dual hydroxylation of L-DOPA at the active site. However, subtle yet significant differences between Edo-Tyr and Bm-Tyr are evident. While Phe261 in Bm-Tyr has been shown to sterically obstruct tyrosine rotation, thereby restricting the orientation of the aromatic ring and limiting access for hydroxylation [46], such steric hindrance is absent in Edo-Tyr, as no equivalent Phe residue appears in its active pocket. This structural difference implies that Edo-Tyr may allow greater conformational freedom of L-DOPA, making tyrosine rotation feasible. Such flexibility could facilitate an electrophilic attack mechanism as proposed by Sani and Malek [37], enabling more efficient hydroxylation of the phenolic substrate. This highlights an important evolutionary distinction between bacterial and fungal tyrosinases: while both conserve critical catalytic residues, fungal tyrosinases like Edo-Tyr may possess a more permissive active site architecture, allowing mechanistic flexibility.

Furthermore, the mode of substrate stabilization also differs. In Bm-Tyr, His208 engages in π–π stacking interactions with the benzene ring of L-DOPA, contributing to aromatic stabilization [46]. By contrast, in Edo-Tyr, His265 forms electrostatic hydrogen bonding interactions with the hydroxyl group of L-DOPA, indicating a shift from aromatic stacking to polar stabilization. This difference may alter the fine-tuning of substrate affinity and turnover rate between bacterial and fungal enzymes. In addition to these catalytic histidines, His90 and Pro277 contribute significantly to substrate stabilization through π–π T-shaped interactions and π–alkyl contacts, respectively. These interactions anchor the aromatic ring within the hydrophobic pocket, enhancing binding affinity and positioning the substrate for catalysis. The contribution of Asp262 through hydrogen bonding further supports substrate orientation, possibly acting as a proton acceptor during the hydroxylation process. Taken together, these results suggest that the catalytic mechanism of Edo-Tyr integrates both conserved and unique

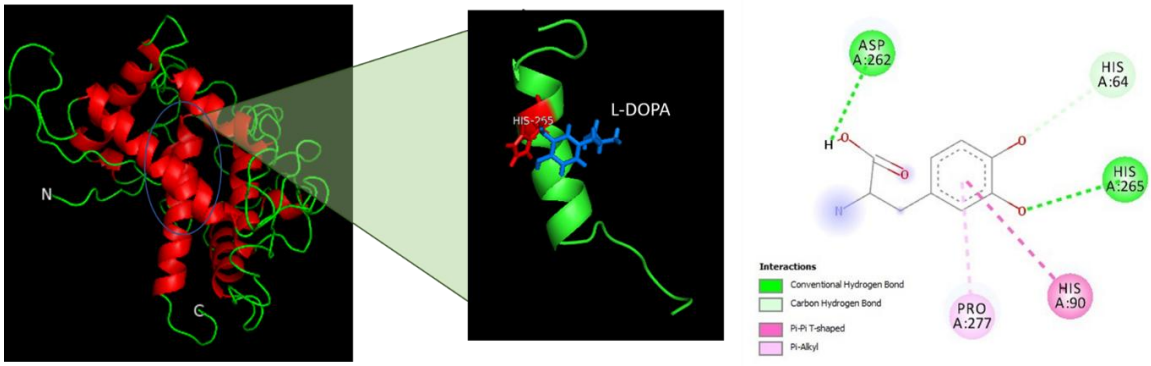

Figure 3. Molecular docking and interaction mapping of Edo-Tyr and L-DOPA substrates with the target enzyme. (Left) The overall 3D structure of the enzyme showing the binding site (highlighted region). (Middle) Docking pose of L-DOPA within the active site, interacting with His-255 residue. (Right) 2D interaction map of Edo-Tyr showing hydrogen bonds (green), carbon-hydrogen bonds (light green), π–π T-shaped interactions (pink), and π–alkyl interactions (magenta) with key amino acid residues

features. Conserved interactions with His64, His265, and Asp262 ensure functional continuity with bacterial tyrosinases, while the absence of steric obstruction from a Phe residue and the altered role of His265 provide Edo-Tyr with enhanced flexibility for substrate orientation and hydroxylation. This dual characteristic supports the theory of divergent evolution with functional conservation, where the catalytic core remains preserved across kingdoms, but variations in peripheral residues modulate efficiency, flexibility, and substrate specificity.

From a theoretical perspective, this observation aligns with the induced-fit model of enzyme catalysis, where the enzyme active site adapts to the conformational dynamics of the substrate, allowing mechanistic flexibility in fungal enzymes. Moreover, the structural divergence between Edo-Tyr and Bm-Tyr provides an example of functional convergence, as both enzymes catalyze the same reaction but employ slightly different molecular strategies for substrate stabilization and catalysis. These insights also imply potential biotechnological applications: the more flexible active site of Edo-Tyr could make it a better candidate for phenolic oxidation in biocatalysis, compared to more rigid bacterial counterparts.

Notably, the application of molecular docking to investigate interactions between tyrosinase and phenolic or phenol-like compounds has been widely reported [47-50]. A substantial number of these studies specifically focus on docking analyses of tyrosinase with L-DOPA, a well-established substrate and intermediate in melanin biosynthesis. Such approaches have provided valuable insights into substrate binding orientation, key interacting residues, and the coordination of copper ions within the active site. These in silico investigations are highly relevant to both biomedical and environmental applications. In the context of melanogenesis, docking studies with L-DOPA and related compounds contribute to understanding the catalytic mechanism of tyrosinase and its role in melanin formation, thereby supporting the development of inhibitors or modulators for cosmetic and dermatological applications. Conversely, from an environmental perspective, the structural similarity between L-DOPA and various phenolic pollutants allows docking studies to serve as predictive tools for assessing the enzyme's potential in phenol degradation and bioremediation. Despite these advances, most existing studies rely on tyrosinase structures from limited sources, and comprehensive analyses involving mushroom-derived tyrosinase, particularly from *L. edodes*, remain scarce. Therefore, integrating molecular docking with structural modeling and experimental validation is essential to better elucidate substrate specificity, catalytic efficiency, and application potential of Edo-Tyr in both melanogenesis-related studies and phenol decontamination pro-

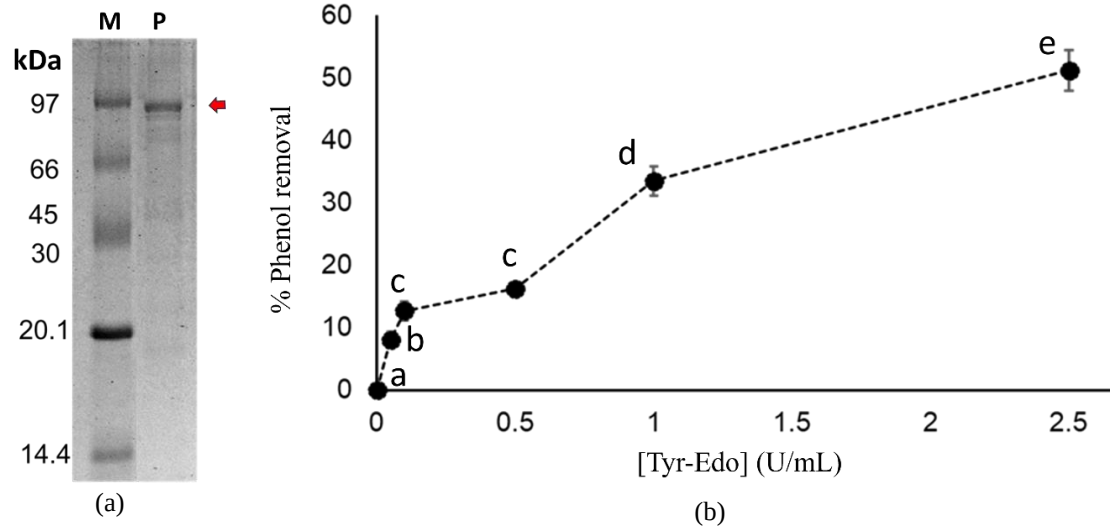

Figure 4. Functional characterization of Edo-Tyr. (A) SDS-PAGE analysis of purified recombinant Edo-Tyr (~95 kDa, including GST tag, indicated by arrow). (B) Phenol degradation assay showing dose-dependent phenol removal. Different letters adjacent to the circles represent statistically significant differences at $p < 0.05$.

cesses.

Although computational predictions indicate that Edo-Tyr is catalytically active, its functional properties have yet to be experimentally confirmed. To investigate this, purified recombinant Edo-Tyr was employed in a phenol degradation assay. As shown in Figure 4a, the SDS-PAGE analysis of Edo-Tyr reveals a high level of purity (>90%), indicating its suitability for the assay. The expected molecular weight of Edo-Tyr is approximately 67 kDa, but it migrates at an apparent size of over 90 kDa on SDS-PAGE. This discrepancy is attributed to the addition of a glutathione S-transferase (GST) tag, which contributes an additional 26 kDa to the protein's N-terminal. Consequently, the total molecular weight of Edo-Tyr with the GST tag is approximately 93 kDa, consistent with the observed size in the SDS-PAGE analysis. Figure 4b illustrates the effect of various tyrosinase concentrations on phenol degradation. The data indicate that tyrosinase reduces phenol concentration in a dose-dependent manner, with significant reduction observed at concentrations above 0.1 U/µL. At tyrosinase concentrations of 0.3 U/µL, approximately 48% of the phenol was removed, leaving 52% of phenol remaining. In this study, 100% phenol corresponds to a concentration of 0.1 mg/mL (see Method section). Therefore, the removal of 48% of phenol corresponds to a reduction of 0.048 mg/mL of phenol. This indicates that for each unit of tyrosinase (0.3 U/µL), the enzyme removes approximately 0.0144 mg/mL of phenol. The IC50 value for phenol removal by tyrosinase was calculated to be 0.36 ± 0.06 U/µL, meaning that 0.36 U/µL of tyrosinase is required to reduce phenol concentration by 0.05 mg/mL from the initial 0.1 mg/mL. The phenol-degrading ability of Edo-Tyr in aqueous solutions has also been previously reported by Wu et al. [51], with several studies demonstrating its use in the enzymatic removal of phenol from wastewater. It is important to note that phenol degradation by Edo-Tyr may vary depending on the initial phenol concentration, a finding supported by Bevilaqua et al. [52], who noted that higher phenol concentrations can regulate the removal efficiency of tyrosinase. Earlier studies, such as Wu et al. [51], also observed a decline in tyrosinase activity as phenol concentration increased. Notably, the experiment employed bovine serum albumin (BSA) as a negative control, which showed no effect on phenol concentration. The use of BSA as a negative control in enzyme assays is well established, as this protein lacks enzymatic activity, as reported in [53–54]. Furthermore, Ilesanmi et al. [55] also confirmed that BSA exhibits no tyrosinase activity. These results therefore validate that Edo-Tyr possesses intrinsic activity in reducing phenol levels in the solution.

While it has been confirmed that the mushroom tyrosinase employed in this study effectively reduced phenol concentrations in the solution, it is imperative to note that the experimental conditions did not involve real wastewater. Instead, an artificial phenol solution was utilized, prepared using Milli-Q water. Consequently, the enzyme's ability to degrade phenol from actual wastewater, such as palm oil mill effluent (POME), remains subject to further verification. Moreover, employing tyrosinase for phenolic degradation often necessitates additional treatments to ensure enzyme stability. The present study utilized free enzyme without immobilization or encapsulation using any additional materials, exposing it to potential risks associated with degradation by external factors, including temperature fluctuations, pH variations, or exposure to other chemical substances. Previous research has demonstrated that immobilized tyrosinase exhibited over 70% degradation efficiency when exposed to an initial phenol concentration of 250 mg/L [56]. Notably, the phenol removal ability of the mushroom tyrosinase in the current study was below 50%, possibly attributable to the enzyme's instability during the process. Further research involving immobilization is evidently warranted to enhance the phenol degradation activity of mushroom tyrosinase. However, it is noteworthy that the activity of the current mushroom tyrosinase in degrading phenolic compounds is comparable to that reported by Wu et al. [51] who achieved approximately 48% degradation. Intriguingly, Wu et al. [51] employed sodium alginate for tyrosinase immobilization, while no immobilization was employed in the current study. This implies that the present mushroom tyrosinase exhibited superior performance compared to the immobilized tyrosinase reported by Wu et al. [51]. Nevertheless, the imperative to enhance the phenolic degradation activity of mushroom tyrosinase warrants further investigation.

Conclusion

The current study reveals the unique structural properties of Edo-Tyr, characterized by a predominance of helical structures and canonical histidine (His) residues serving as active sites. A Cu^{2+} ion was observed in the structure, apparently coordinated by seven His residues. Molecular docking analysis further suggests that the catalytic mechanism of Edo-Tyr involves tyrosinase rotation, stabilization through π-π or π-alkyl interactions by His residues, followed by an electrostatic attack on the hydroxyl group of the L-DOPA substrate. Additionally, the study confirms that Edo-Tyr can degrade phenol in solution in a concentration-dependent manner. These findings highlight the potential applications of recombinant Edo-Tyr in bioremediation, particularly for the removal of phenolic contaminants from wastewater.

Acknowledgement

We gratefully acknowledge Universiti Malaysia Sabah for supporting this research under the Skim Dana Niche grant (DN20083) and GUG0531-2/2020. The authors also thank Sumiyane Arifah Sufiyan for her valuable technical assistance in the phenolic assay experiments.

References

1. Qu Y, Zhan Q, Du S et al. (2020) Catalysis-based specific detection and inhibition of tyrosinase and their application. Journal of Pharmaceutical Analysis 10(5):414–425. doi:10.1016/j.jpha.2020.07.004
2. Capasso C, Supuran CT (2024) Carbonic anhydrase and bacterial metabolism: a chance for antibacterial drug discovery. *Expert Opinion on Therapeutic Patents* 34(6):465–474. doi:10.1080/13543776.2024.2332663
3. Xu W, Bai M, Du NN et al. (2022) Chemical structures and anti-tyrosinase activity of the constituents from *Elephantopus scaber* L. Fitoterapia 162:105259. doi:10.1016/j.fitote.2022.105259
4. Weissman DH, Jiang J, Egner T (2014) Determinants of congruency sequence effects without learning and memory confounds. Journal of Experimental Psychology: Human Perception and Performance 40(5):2022–2037. doi:10.1037/a0037454
5. Sachan P, Madan S, Hussain A (2019) Isolation and screening of phenol-degrading bacteria from pulp and paper mill effluent. Applied Water Science 9(5):100. doi:10.1007/s13201-019-0989-4
6. Saha NC, Bhunia F, Kaviraj A (1999) Toxicity of phenol to fish and aquatic ecosystems. Bulletin of Environmental Contamination and Toxicology 63(2):195–202
7. Mhlongo NL, Akharame MO, Pereao O et al. (2024) Phenolic compounds occurrence and human health risk assessment in potable and treated waters in Western Cape, South Africa. Frontiers in Toxicology 5:1269601. doi:10.3389/ftox.2023.1269601
8. Pretzler M, Rompel A (2024) Tyrosinases: a family of copper-containing metalloenzymes. ChemTexts 10(4):12. doi:10.1007/s40828-024-00195-y
9. Noh H, Lee SJ, Jo HJ et al. (2020) Histidine residues at the copper-binding site in human tyrosinase are essential for its catalytic activities. Journal of Enzyme Inhibition and Medicinal Chemistry 35(1):726–732. doi:10.1080/14756366.2020.1740691
10. Goldfeder M, Kanteev M, Isaschar-Ovdat S et al. (2014) Determination of tyrosinase substrate-binding modes reveals mechanistic differences between type-3 copper proteins. Nature Communications 5:4505. doi:10.1038/ncomms5505
11. Xu H, Han G, Li Y, Meng Q et al. (2025) Enhancing yield and quality: research and practice of agro-forest waste for Lentinus edodes (shiitake mushroom) cultivation. Frontiers in Nutrition 12:1538039. doi:10.3389/fnut.2025.1538039
12. Foo SF, Saikim FH, Kulip J, Sathiya Seelan JS (2018) Distribution and ethnomycological knowledge of wild edible mushrooms in Sabah (Northern Borneo), Malaysia. Journal of Tropical Biology and Conservation 15:203–222. doi:10.51200/jtbc.v15i0.1494
13. Chan PT, Matanjun P, Budiman C et al. (2022) Novel peptide sequences with ACE-inhibitory and antioxidant activities derived from the heads and bones of hybrid groupers (*Epinephelus lanceolatus* × *Epinephelus fuscoguttatus*). *Foods* 11(24):3991. doi:10.3390/foods11243991
14. Fujieda N, Umakoshi K, Ochi Y et al. (2020) Copper–oxygen dynamics in the tyrosinase mechanism. Angewandte Chemie International Edition 59(32):13385–13390. doi:10.1002/anie.202004733
15. Waterhouse A, Bertoni M, Bienert S et al. (2018) SWISS-MODEL: homology modelling of protein structures and complexes. Nucleic Acids Research 46(W1):W296–W303. doi:10.1093/nar/gky427
16. Powell HR, Islam SA, David A, Sternberg MJE (2025) Phyre2.2: a community resource for template-based protein structure prediction. Journal of Molecular Biology 437(15):168960. doi:10.1016/j.jmb.2025.168960
17. Zheng W, Zhang C, Bell EW, Zhang Y (2019) I-TASSER gateway: a protein structure and function prediction server powered by XSEDE. Future Generation Computer Systems 99:73–85. doi:10.1016/j.future.2019.04.011
18. Ogunjobi TT, Okorie IC, Gigam-Ozuzu CD et al. (2025) Bioinformatics tools in protein analysis: structure prediction, interaction modelling, and function relationship. European Journal of Sustainable Development Research 9(3):em0298. doi:10.29333/ejosdr/1634
19. Santhoshkumar R, Yusuf A (2020) In silico structural modeling and analysis of physicochemical properties of curcumin synthase (CURS1, CURS2, and CURS3) proteins of Curcuma longa. Journal of Genetic Engineering and Biotechnology 18(1):24. doi:10.1186/s43141-020-00052-5
20. Waterhouse AM, Studer G, Robin X et al. (2024) The structure assessment web server: for proteins, complexes and more. Nucleic Acids Research 52(W1):W318–W323. doi:10.1093/nar/gkae270

21. Hiếu T, Thiên Đ, Liêm L, Minh Thường N (2024) Protein structure modeling using cloud-based servers. VNUHCM Journal of Natural Sciences 8(1):2828–2837. doi:10.32508/stdjns.v8i1.1244
22. Nusantoro YR, Fadlan A (2021) The effect of energy minimization on the molecular docking of acetone-based oxindole derivatives. JKPK (Jurnal Kimia dan Pendidikan Kimia) 6(1):69–77
23. Ozvoldik K, Stockner T, Krieger E (2023) YASARA Model: interactive molecular modeling from two dimensions to virtual realities. Journal of Chemical Information and Modeling 63:6177–6182. doi:10.1021/acs.jcim.3c01136
24. Orobitg M, Guirado F, Cores F et al. (2015) High performance computing improvements on bioinformatics consistency-based multiple sequence alignment tools. Parallel Computing 42:18–34. doi:10.1016/j.parco.2014.12.002
25. Zhang C, Wang Q, Li Y et al. (2024) The historical evolution and significance of multiple sequence alignment in molecular structure and function prediction. Biomolecules 14:1531. doi:10.3390/biom14121531
26. Lindang HU, Budiman C (2022) Structural and substrate interaction properties of alkaline phosphatase from Paenibacillus sp. PSB04: in silico analysis. OnLine Journal of Biological Sciences 22(3):256–267. doi:10.3844/ojbsci.2022.256.267
27. Duvaud S, Gabella C, Lisacek F et al. (2021) Expasy, the Swiss Bioinformatics Resource Portal, as designed by its users. Nucleic Acids Research 49(W1):W216–W227. doi:10.1093/nar/gkab225
28. Goh CKW, Silvester J, Wan Mahadi WNS et al. (2018) Expression and characterization of functional domains of FK506-binding protein 35 from Plasmodium knowlesi. Protein Engineering, Design and Selection 31(12):489–498. doi:10.1093/protein/gzz008
29. Koshkina MK, Shelomov MD, Pometun AA et al. (2023) Speeding up SDS–PAGE: theory and experiment. Electrophoresis 44(15–16):1155–1164. doi:10.1002/elps.202300011
30. Zhang XW, Bian GL, Kang PY et al. (2021) Recent advance in the discovery of tyrosinase inhibitors from natural sources via separation methods. Journal of Enzyme Inhibition and Medicinal Chemistry 36(1):2104–2117. doi:10.1080/14756366.2021.1983559
31. Ilang NI, Goh CKW, Arifin M, Budiman C (2025) Interplay between collagen hydrolysates and the ability of FKBP35 from *Plasmodium knowlesi* in preventing insulin aggregation. Sains Malaysiana 54(5):1269–1280. doi:10.17576/jsm-2025-5405-06
32. Razali R, Kumar V, Budiman C (2023) Tenderness and physicochemical characteristics of meat treated by recombinant bromelain of MD2 pineapple from a codon-optimized synthetic gene. Emirates Journal of Food and Agriculture 35(10). doi:10.9755/ejfa.2023.3164
33. Ismaya WT, Tandrasasmita OM, Sundari S et al. (2017) The light subunit of mushroom *Agaricus bisporus* tyrosinase: its biological characteristics and implications. International Journal of Biological Macromolecules 102:308–314
34. Duthoo E, Delroisse J, Maldonado B et al. (2024) Diversity and evolution of tyrosinase enzymes involved in the adhesive systems of mussels and tubeworms. iScience 27(12):111443. doi:10.1016/j.isci.2024.111443
35. Shakil M, Harlalka GV, Ali S et al. (2019) Tyrosinase (TYR) gene sequencing and literature review reveals recurrent mutations and multiple population founder gene mutations as causative of oculocutaneous albinism (OCA) in Pakistani families. Eye (London) 33(8):1339–1346. doi:10.1038/s41433-019-0436-9
36. Lin HC, Li WH, Chen CC et al. (2020) Diverse enzymes with industrial applications in four thraustochytrid genera. Frontiers in Microbiology 11:573907. doi:10.3389/fmicb.2020.573907
37. Sani NS, Malek NANN (2023) Immobilization of tyrosinase and its application. Journal of Materials in Life Sciences 2(1):73–81. doi:10.11113/jomalisc.v2.16
38. Lai X, Wichers HJ, Soler-Lopez M, Dijkstra BW (2017) Structure of human tyrosinase related protein 1 reveals a binuclear zinc active site important for melanogenesis. Angewandte Chemie International Edition 56(33):9812–9815. doi:10.1002/anie.201704616
39. Oyama T, Yoshimori A, Ogawa H et al. (2022) The structural differences between mushroom and human tyrosinase clarified by investigating the inhibitory activities of stilbenes. Journal of Molecular Structure 1272:134180. doi:10.1016/j.molstruc.2022.134180
40. Fekry M, Dave KK, Badgujar D et al. (2023) The crystal structure of tyrosinase from *Verrucomicrobium spinosum* reveals it to be an atypical bacterial tyrosinase. Biomolecules 13(9):1360. doi:10.3390/biom13091360
41. DuPai CD, Davies BW, Wilke CO (2021) A systematic analysis of the beta hairpin motif in the Protein Data Bank. Protein Science 30(3):613–623. doi:10.1002/pro.4020
42. Tsai TY, Lee YHW (1998) Roles of copper ligands in the activation and secretion of *Streptomyces* tyrosinase. *Journal of Biological Chemistry* 273(30):19243–19250. doi:10.1074/jbc.273.30.19243
43. Noh H, Lee SJ, Jo HJ et al. (2020) Histidine residues at the copper-binding site in human tyrosinase are essential for its catalytic activities. Journal of Enzyme Inhibition and Medicinal Chemistry 35(1):726–732. doi:10.1080/14756366.2020.1740691
44. Decker H, Schweikardt T, Nillius D et al. (2007) Similar enzyme activation and catalysis in hemocyanins and tyrosinases. Gene 398(1–2):183–191. doi:10.1016/j.gene.2007.02.051
45. Kampatsikas I, Pretzler M, Rompel A (2020) Identification of amino acid residues responsible for C–H activation in type-III copper enzymes by generating tyrosinase activity in a catechol oxidase. Angewandte Chemie International Edition 59(47):20940–20945. doi:10.1002/anie.202008859
46. Rolff M, Schottenheim J, Decker H, Tuczek F (2011) Copper–O_2 reactivity of tyrosinase models towards external monophenolic substrates: molecular mechanism and comparison with the enzyme. Chemical Society Reviews 40(7):4077. doi:10.1039/c0cs00202j
47. Nazir Y, Rafique H, Roshan S et al. (2022) Molecular docking, synthesis, and tyrosinase inhibition activity of acetophenone amide: potential inhibitor of melanogenesis. BioMed Research International 2022:1040693. doi:10.1155/2022/1040693
48. da Silva AP, Silva NF, Andrade EHA et al. (2017) Tyrosinase inhibitory activity, molecular docking studies and antioxidant potential of chemotypes of *Lippia ori-*

ganoides essential oils. PLoS One 12(5):e0175598. doi:10.1371/journal.pone.0175598
49. Feng YX, Wang ZC, Chen JX et al. (2021) Separation, identification, and molecular docking of tyrosinase inhibitory peptides from the hydrolysates of defatted walnut (*Juglans regia* L.) meal. Food Chemistry 353:129471. doi:10.1016/j.foodchem.2021.129471
50. Sripadung P, Rajchakom C, Nunthaboot N et al. (2025) Computational and experimental insights into tyrosinase and antioxidant activities of resveratrol and its derivatives: molecular docking, molecular dynamics simulation, DFT calculation, and in vitro evaluation. International Journal of Molecular Sciences 26:8827. doi:10.3390/ijms26188827
51. Wu X, Li X, Li H et al. (2017) A highly sensitive and selective fluorescence off–on probe for the detection of intracellular endogenous tyrosinase activity. Chemical Communications 53(16):2443–2446. doi:10.1039/c6cc09679d
52. Bevilaqua JV, Cammarota MC, Freire DMG, Sant'Anna GL Jr (2002) Phenol removal through combined biological and enzymatic treatments. Brazilian Journal of Chemical Engineering 19(2):151–158. doi:10.1590/S0104-66322002000200010
53. Razali R, Budiman C, Kamaruzaman KA, Subbiah VK (2021) Soluble expression and catalytic properties of codon-optimized recombinant bromelain from MD2 pineapple in *Escherichia coli*. Protein Journal 40(3):406–418. doi:10.1007/s10930-021-09974-9
54. Razali R, Subbiah VK, Budiman C (2021) Technical data of heterologous expression and purification of SARS-CoV-2 proteases using *Escherichia coli* system. Data 6:99. doi:10.3390/data6090099
55. Ilesanmi OS, Adedugbe OF, Adewale IO (2021) Potentials of purified tyrosinase from yam (*Dioscorea* spp.) as a biocatalyst in the synthesis of cross-linked protein networks. Heliyon 7(8):e07831. doi:10.1016/j.heliyon.2021.e07831
56. Abdollahi K, Yazdani F, Panahi R, Mokhtarani B (2018) Biotransformation of phenol in synthetic wastewater using the functionalized magnetic nano-biocatalyst particles carrying tyrosinase. 3 Biotech 8(10):419. doi:10.1007/s13205-018-1445-2

This page is intentionally left blank.